communications earth & environment

Article

A Nature Portfolio journal

https://doi.org/10.1038/s43247-026-03395-1

Climate change reduces pelagic biomass in a coastal upwelling ecosystem

Lucas T. Nunes[1] ✉, Thiago da S. Matos[1], Carolina Reis[1], Yuri Artioli[2], Guillem Chust[3], Andressa Claudio[1], Ricardo Coutinho[1], Carlos E. L. Ferreira[4], Patrizio Mariani[5] & Lohengrin Fernandes[1]

Global fisheries rely heavily on oceanic primary and secondary productivity. However, how regional food webs will respond to ongoing climate change—and the resulting implications for fish biomass—remains poorly understood. Coastal upwelling systems are among the most biologically productive regions on Earth. Their responses to warming are often non-linear and vary by region, making it essential to examine them in detail to anticipate ecosystem-level impacts. Here we used a machine learning framework to project future changes in marine community dynamics, scaling from nutrient speciation to fish biomass. While recycled nitrogen forms (ammonium) are projected to increase, a long-term decline in new nitrogen inputs (nitrate) is associated with reduced phytoplankton growth and fish biomass, particularly under high-emission scenarios. Our findings highlight the critical benefits of pursuing low greenhouse gas emission pathways to limit fishery declines and support the resilience and partial recovery of upwelling ecosystems in a warming ocean.

Temperature and nutrients are known to influence individual metabolism, species distribution, and ecosystem dynamics across multiple trophic levels[1,2]. Rising environmental temperature can be particularly detrimental to ectothermic organisms, leading to demographic changes in community structure by decreasing species' abundance and/or biomass[3], decreasing trophic transfer efficiency[3,4], skewing organisms body size[5,6], and accelerating species' consumption rates and energetic demands[2,7]. Similarly, nutrient availability and speciation shape communities, often favouring species with greater niche breadth and lower nutritional requirements[1,8]. Under current scenarios of ongoing global changes, understanding the interplay between sea temperature and nutrient availability at different spatial and temporal scales is mandatory to better predict energy flow and threats to marine ecosystems[4,9].

Coastal upwelling systems hold high socioeconomic importance due to their large biomass stocks of commercially targeted species[10]. These systems are driven by the enrichment of surface waters with macro- and micronutrients from the deep ocean, following a temporary break-up of vertical thermohaline stratification and the deepening of the Mixed Layer Depth[11] (MLD). These incoming nutrients fuel bottom-up processes and primary production rates, but their effects on producer dynamics and ecosystem productivity are not always linear[12–14]. Changes in upwelling intensity under extreme climate change scenarios vary considerably between regions, emphasising the need to study each system individually to accurately predict ecosystem-level consequences[14]. Also, annual-mean upwelling often fails to capture crucial seasonal variations and long-term trends in upwelling intensity, which are critical for understanding nutrient transport and primary productivity[14]. Intensified upwelling events can favour larger phytoplankton and zooplankton species, which thrive in low temperatures and high nutrient availability[15,16], resulting in enhanced energy transfer to higher trophic levels, including fish and marine mammals. Conversely, diminished upwelling intensity in some regions may lead to declines in biological productivity, underscoring the complex and region-specific nature of climate impacts.

Cascade bottom-up processes, such as the rising in phytoplankton biomass after nutrient inputs due to upwelling, are well-known for favouring energy flow and thus regulating marine fish production[17–23]. Less well-documented is how the warming-induced changes in upper layers of the ocean could cascade throughout the nutrient supply and plankton stocks, up to large consumers at the higher trophic levels. Our approach aims to reveal how upwelling ecosystems may respond to temperature changes and nutrient availability over time, under different Earth System Model climate scenarios, by examining ocean warming impacts on bottom-up processes from nutrient inputs to fishery landings. We thus applied supervised machine learning methods to time-series data from the Cabo

[1]Marine Biotechnology, Instituto de Estudos do Mar Almirante Paulo Moreira, Arraial do Cabo, RJ, 28930-000, Brazil. [2]Plymouth Marine Laboratory, Plymouth, PL1 3DH, UK. [3]AZTI Marine Research, Basque Research and Technology Alliance (BRTA), Txatxarramendi Ugartea z/g, 48395 Sukarrieta, Spain. [4]Reef Systems Ecology and Conservation Lab, Universidade Federal Fluminense, Niterói, RJ, 24210-201, Brazil. [5]National Institute of Aquatic Resources, Technical University of Denmark, Henrik Dams, 201, 2800 Kongens Lyngby, Denmark. ✉e-mail: nuneslteixeira@gmail.com

Frio region, one of the most important upwelling systems along the eastern coast of South America. We hypothesised high temperatures, expected under extreme climate change scenarios, would decrease pelagic production and consequently diminish fishery yields over time (Fig. 1). Therefore, by analysing these interactions over a long temporal scale, we can establish a framework to more accurately predict the future impacts of rising environmental temperatures on marine community dynamics and fisheries production.

We demonstrate that ocean warming is likely to drive pronounced bottom-up changes in the Cabo Frio upwelling system. Across future scenarios, warming leads to declines in phytoplankton and fish biomass, particularly under high-emission pathways, with projected losses reaching up to 78% by 2100. In contrast, the low-emission scenario indicates partial stabilization and signs of ecosystem recovery after mid-century, underscoring the importance of sustainable climate trajectories for maintaining pelagic productivity and fisheries resilience.

Results

Historical and projected sea surface temperature

Projected future warming scenarios derived from the Coupled Model Intercomparison Project Phase 6 - CMIP6[24] represent divergent development pathways until 2100, ranging from sustainable (SSP1-2.6) to a higher emissions scenario with moderate mitigation efforts (SSP3-7.0), and extending further to a fossil-fuel-dependent pathway (SSP5-8.5). The historical average in situ sea surface temperature from 2005 to 2016 was 22.2 °C ± 1.4 °C (mean ± SD; Fig. 2a, black dashed line). The historical temperature exhibited an initial trend (23.0 ± 1.6 °C in 2010) comparable to the early stages of the CMIP6 future projections (23.3 ± 1.7 °C in 2017; Supplementary Fig. 1). However, a marked temperature decrease was observed in 2011, followed by an increase in 2015 and 2016. This substantial variation between 2010 and 2014 may be attributed to the strong La Niña events during these years, which likely caused cooling of the regional waters[25]. After 2017, the three CMPI6 projections follow a similar increasing trend until approximately 2060, after which SSP1-2.6 stabilises near 24 °C (Fig. 2a, green line), while SSP3-7.0 and SSP5-8.5 projections point towards a higher temperature in 2100 (26 °C) (Fig. 2a, red and blue lines).

Ecosystem responses to warming

Nitrogen, an essential nutrient either in the form of nitrate or ammonia, is critical for the growth and reproduction of phytoplankton, playing a key role in primary productivity[1,26]. Our model estimated historical (2005–2016) mean concentrations of 0.56 ± 0.2 µM for nitrate, 1.32 ± 0.23 µM for ammonia, and 0.23 ± 0.04 µM for phosphate (Supplementary Figs. 2; 3 and 4). At the start of the projections (2017), the largest reduction in nitrate concentration occurred under SSP5-8.5, with a 9% decrease to 0.51 ± 0.13 µM. By 2100, the lowest nitrate concentration was projected under SSP3-7.0, reaching 0.37 ± 0.14 µM (Fig. 2b). In contrast, ammonia concentrations were projected to increase, starting at 1.39 ± 0.22 µM (a 5.3% increase) under SSP1-2.6 in 2017 and rising to 1.65 ± 0.19 µM (a 26% increase) by 2100 (Fig. 2c). Phosphate concentrations slightly decreased to 0.22 ± 0.03 µM (a 4.4% reduction) at the beginning of the projections across all scenarios and could decline by up to 26%, reaching 0.17 ± 0.02 µM under SSP3-7.0 by the end of the century (Fig. 2d).

Along with SST, current nitrate levels are key drivers of phytoplankton biomass. The projected decrease in nitrate concentrations over time likely contributes to the decline in phytoplankton biomass, with historical estimates of 240 ± 48 mgC m^{-3} decreasing by 1.37% (to 239 ± 33 mgC m^{-3} under SSP1-2.6) in 2017, and by 22% (to 187 ± 10 mgC m^{-3}) under SSP3-7.0 in 2100 (Fig. 3). This reduction is particularly evident under SSP5-8.5 scenario and coincides with a shift in nitrogen sources towards ammonia, especially considering the lagged effect of this nutrient on phytoplankton growth (Supplementary Fig. 5). The imbalance between nitrogen sources, combined with decreasing phosphate concentrations, may sustain some level of phytoplankton growth despite lower nitrate availability, while potentially favouring different taxonomic groups.

Seston biomass historically averaged 63 ± 31 mgC m^{-3}. Across all scenarios, a modest but steady increase in biomass is projected throughout the century that likely contributes to controlling the phytoplankton growth (Fig. 3). In 2017, an increase of 19% (75 ± 16 mgC m^{-3}) is expected under SSP1-2.6. The largest increase (~42%) is projected under SSP3-7.0, reaching 89 ± 17 mgC m^{-3} by the end of the century. Notably, seston biomass showed a sharp reduction in 2016, with a similar decline observed in 2006 (Supplementary Fig. 6), suggesting that long-term time series are essential to capture potential decadal or longer-term fluctuations.

Fish biomass also declined in 2016 (Fig. 3), likely reflecting the combined effects of sea surface temperature (SST) and seston availability (Supplementary Fig. 7). Historical data indicate an average fish biomass of 16,029 ± 9,492 mg m^{-2} (or 160.3 kg ha^{-1}; Fig. 3). At the beginning of the projections, we observed a 39% reduction under SSP3-7.0, reaching 9,850 ± 7,675 mg m^{-2} (or 98.5 ± 76.8 kg ha^{-1}). By the end of the century, it is projected to decline by up to 78%, reaching 3,486 ± 431 mg m^{-2} (or 34.9 ± 4.3 kg ha^{-1}). Fish biomass also showed the greatest initial decline among the variables analysed, as evidenced by the sharp reduction at the onset of the projections. This pattern is clearly illustrated when comparing the predicted and observed values (Supplementary Fig. 8), highlighting the substantial drop and the high variability captured by the model.

Trends and breaking points in ecosystem projections

All variables, except fish biomass under the SSP1-2.6 scenario, exhibited significant non-linear trends, with Tau values ranging from 0.1 to 0.4 (Fig. 4; Supplementary Table 1). Most variables showed strong oscillations from the beginning of the projections up to the first identified breakpoint, which

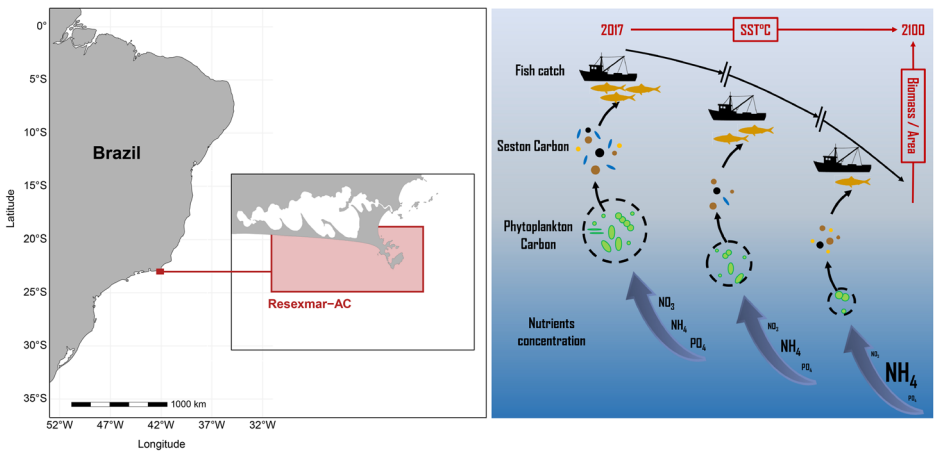

Fig. 1 | Study area and conceptual hypothesis. The study focuses on the Upwelling Region of Resexmar-AC, located off the southeastern coast of Brazil. Under future warming scenarios, we hypothesise a decline in ecosystem biomass driven by rising sea surface temperatures and changes in nutrient concentrations. The conceptual diagram illustrates the expected cascading effects, from nutrient availability (NO_3^-, NH_4^+, PO_4^{3-}) to phytoplankton, seston, and ultimately fish biomass.

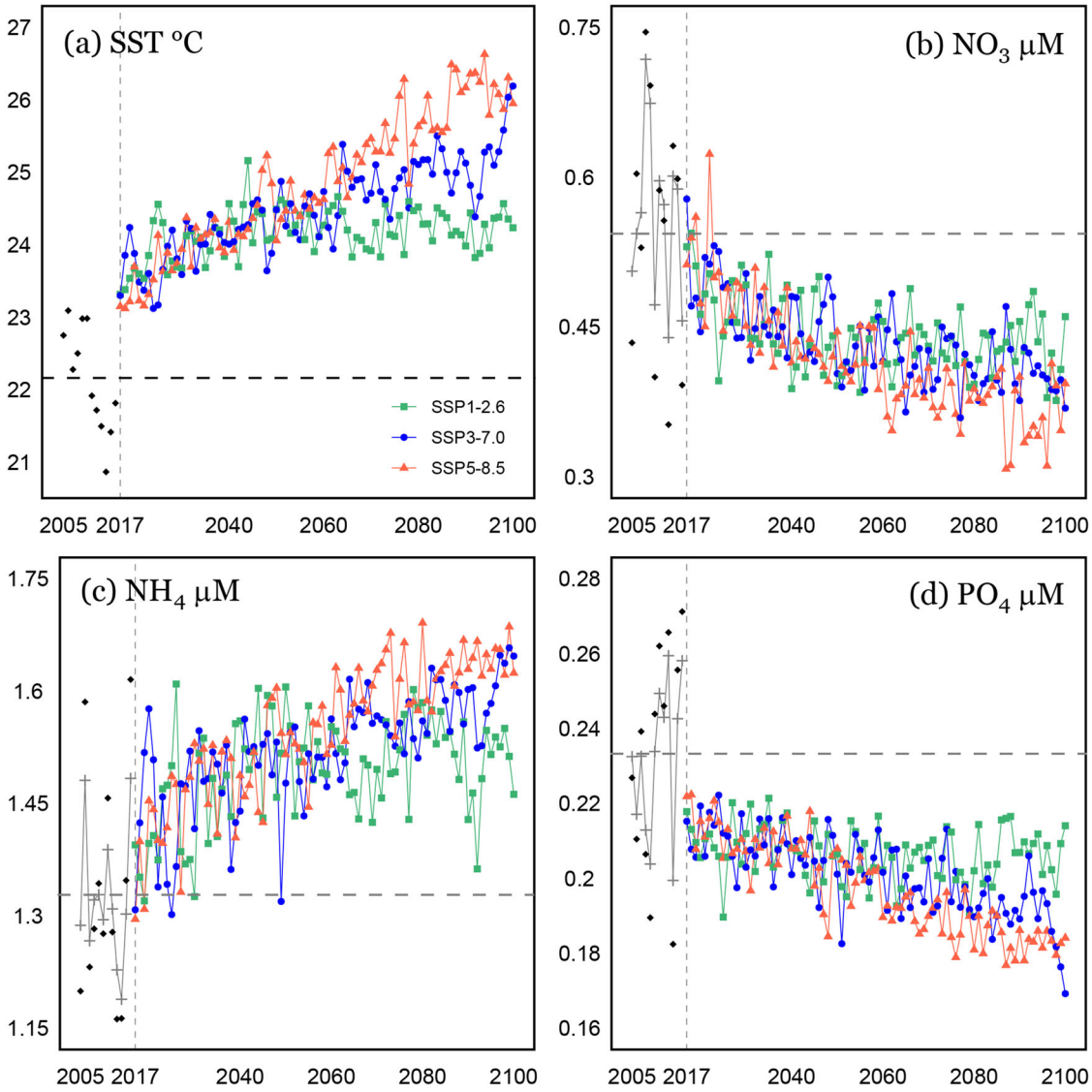

Fig. 2 | Temperature and nutrient responses to warming scenarios. a CMIP6-derived temperatures for future warming scenarios (coloured) alongside in situ measurements (black diamonds), with the black line representing the historical average. Nutrient concentrations (micromolar) over time for (**b**) nitrate, (**c**) ammonia, and (**d**) phosphate. The vertical grey dashed line marks the transition from observed to predicted values, while the horizontal grey dashed line indicates the historical (2005–2016) modelled nutrient averages. Lines and points represent annual averages for historical model-adjusted values (grey) and predicted values (coloured).

occurred between 2033 and 2050 (Fig. 4). This pattern is consistent with an initial transition period under rapidly changing climate forcing, followed by a phase of relative stabilisation or reduced amplitude of fluctuations in subsequent years (Fig. 5). Trends confirm a significant initial decline in nitrate across all scenarios, particularly under SSP1-2.6, followed by stabilisation. Ammonium exhibited a positive trend until approximately 2048, continuing to increase gradually until 2100. Phosphate showed a steady declining trend throughout the century, with a sharper decrease under SSP3-7.0. Fish biomass displayed the most pronounced fluctuations, with a steep initial drop followed by persistent variability and wide amplitude changes in later periods (Fig. 4). This pattern is reinforced by the high variability in fish biomass captured by the model (Supplementary Fig. 8). Heatmap analysis (Fig. 5) illustrates this pattern of ecosystem instability at the beginning of the projections, with more frequent and intense deviations observed across variables, especially for nitrate and fish biomass. Under SSP3-7.0 and SSP5-8.5, the concentration of these deviations remains higher throughout the century, suggesting sustained system variability under more severe climate scenarios.

Discussion

We showed a marked sensitivity to climate change in the Cabo Frio upwelling system, with an initial period of strong oscillations in both the magnitude and frequency of nutrients and fish biomass. Similar patterns of climate sensitivity have also been observed in other upwelling systems worldwide[13,27], suggesting that such responses may be characteristic of these highly dynamic ecosystems. These fluctuations were particularly high under extreme warming scenarios until the 2030 s. After this period, however, model-derived trends begin to diverge, indicating that ecosystem stability is more likely only under the lower-emission pathway (SSP1-2.6). In contrast, under high-emission trajectories, changes from the historical period are expected to remain pronounced by the end of the century, driven by bottom-up effects, as temperature and nutrient shifts cascade through the upwelling food web[28].

The most substantial alterations in marine ecological parameters in our study region are anticipated by approximately 2050. Marine models already highlight increasing divergence among warming scenarios after approximately 2060, particularly for higher trophic levels, where elevated

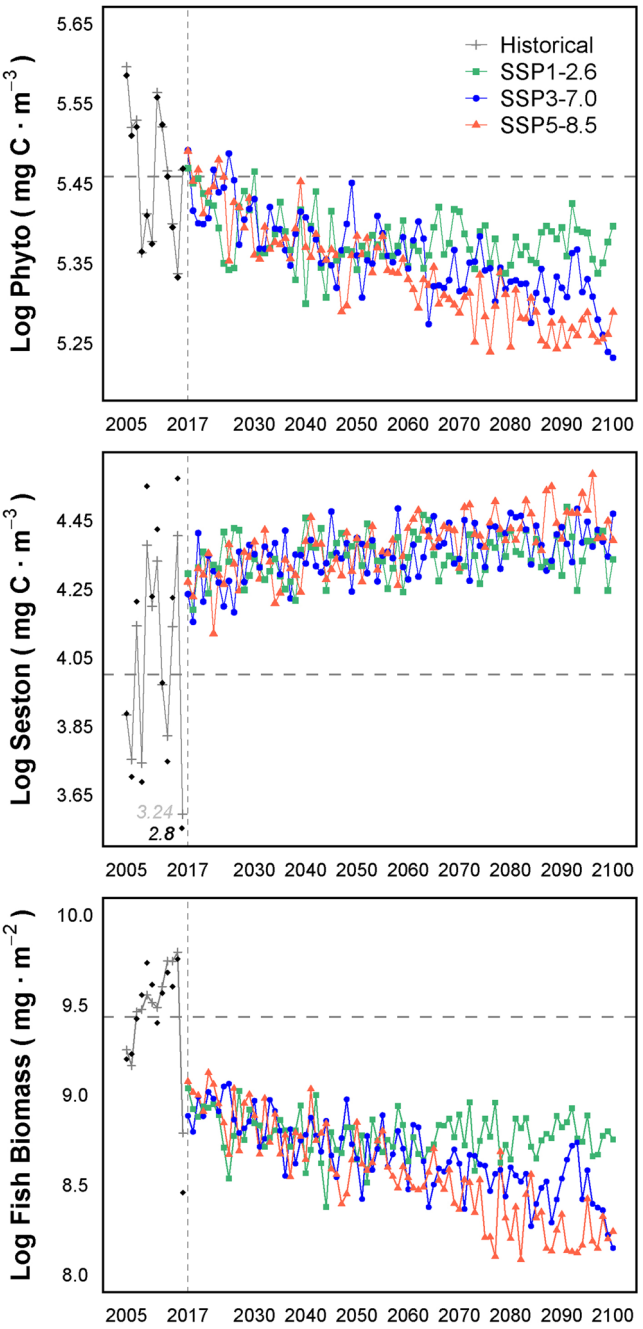

Fig. 3 | Impact of present and warming scenarios on phytoplankton (Log mgC m^{-3}), Seston (Log mgC m^{-3}) and Fish Biomass (Log mg m^{-2}). Black diamonds represent measured annual averages. Lines and points show the annual averages for historical model-adjusted values (grey) and predicted values (coloured). Vertical grey dashed line denotes the transition from observed data (2005 to 2016) to predicted values (2017 to 2100). Horizontal grey dashed line represents the historical (2005-2017) average for each parameter.

temperatures may exceed species' thermal niches[3,29]. These results highlight the need for regional studies, as different ecosystems exhibit contrasting nonlinear responses to warming[14,21,28,30], which is crucial for effective conservation strategies. Additionally, the use of a decade-long weekly time series enhances the model's ability to predict relationships across successive ecosystem compartments, and provides the basis for evaluating long-term trajectories of ecosystem stability across future scenarios.

Our results further demonstrate that under the sustainable SSP1-2.6 pathway, the system exhibits signs of ecological recovery. After an initial disturbance, indicated by the first breakpoints in the time series, trajectories of nutrients, phytoplankton, seston, and fish biomass stabilize, with slopes approaching zero by the end of the century. This stabilization does not imply a full return to historical conditions, but rather reflects the capacity of the ecosystem to re-stabilize under reduced warming. In contrast, under SSP3-7.0 and SSP5-8.5, trends remain strongly directional throughout the century, suggesting ongoing deterioration. These findings emphasize that sustainable pathways can mitigate impacts and preserve ecosystem resilience, while higher-emission scenarios result in persistent losses.

Although our models demonstrated robustness, as indicated by performance metrics MAE and RMSE (see Supplementary Figs.), we acknowledge that our projections are based on a single CMIP6 model, the NorESM2-MM. However, this model was selected after a detailed comparison with the ensemble of all available CMIP6 models for our study area, where it showed a high correlation with the ensemble median across all scenarios (Supplementary Fig. 9). This supports the representativeness of the NorESM2-MM for our regional projections, minimising the risk of warming bias. Nonetheless, we recognise that using a single Earth System Model may still introduce uncertainties, especially regarding the range of possible outcomes and the complexity of fish population movements linked to upwelling seasonality. We recommend future studies incorporate multi-model ensembles to further reduce model dependency and better capture uncertainty ranges.

Our findings of a decrease in phytoplankton and fish biomass, coupled with an increase in seston biomass, align with observed patterns in various ecosystems, such as tropical atoll systems[3], the subarctic Barents Sea system[28], and a past study in the same system of Cabo Frio Upwelling[31]. The decline in phytoplankton and fish biomass over time due to warming is a globally common pattern, with several studies reporting similar trends across diverse marine environments[21,28]. These parallels reinforce the cascading effects of warming on food web restructuring, particularly the microbialization of energy pathways and altered nutrient recycling[32]. High concentrations of ammonia, coupled with warm temperatures, accelerate the nitrification process in coastal waters and may fuel ocean microbialization[32], favouring suspension-feeding zooplankton and invertivorous fishes[3]. On one side, the increase in large zooplankton abundance enhances top-down control on phytoplankton, while small picoplankton cells—with high surface area-to-volume ratios—such as ammonia-oxidizing archaea and bacteria, simultaneously outcompete phytoplankton for ammonium and other nutrients[33]. Despite its inherent simplifications, our model captured key ecological responses to warming, offering insights that align with both empirical and theoretical work. This alignment underscores the potential utility of such models in forecasting and mitigating the impacts of global climate change on marine ecosystems.

We also emphasise the importance of describing and predicting the coupling of pelagic community biomasses, particularly in the context of climate changes. These communities are highly diverse, span multiple trophic levels, and include organisms and particles of varying sizes, from plankton to fish, making them inherently complex to study. Previous studies have examined the impacts of warming on the phyto and zooplankton community, revealing substantial shifts in composition and biomass[29,34] and underscoring the need for further investigation into their ecological dynamics. Increased stratification, driven by warming, plays a key role in shaping these changes, particularly by altering the dynamics between phytoplankton and zooplankton[35]. As warming progresses, its impact on plankton communities could extend beyond shifts in species composition, by affecting broader ecological processes such as nutrient cycling and the structure of the pelagic food web.

Like most zooplankton biomass studies, our model considers seston as a key component of these changes, as it encompasses both organisms and particulate organic matter[36–38] (POM). Additionally, Bayesian isotopic models have shown that POM is essential for sustaining pelagic primary consumers, further underscoring its critical role in marine ecosystems[39,40]. As warming scenarios progress, the composition of seston can shift, with a transition from zooplankton dominance to an increase presence of detritus.

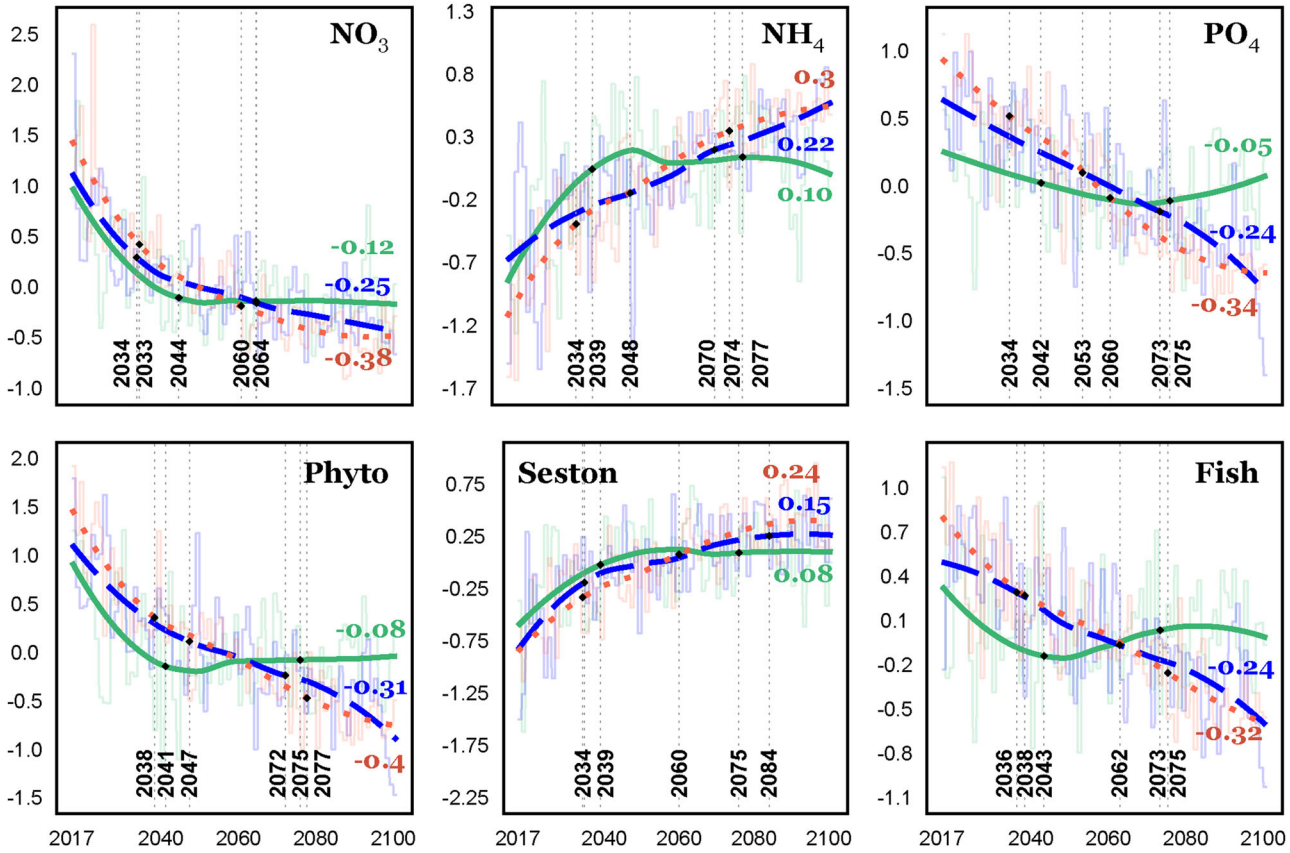

Fig. 4 | Standardised trends over future warming scenarios. Coloured lines represent annual averages of standardised *z*-scores (Loess regression) for each variable under future climate scenarios: SSP1-2.6 (solid green line), SSP3-7.0 (dashed blue line), and SSP5-8.5 (dotted red line). Standardisation was performed by removing seasonality through *z*-score normalisation within each month and each scenario. Positive values indicate deviations above the monthly mean within the respective scenario, and negative values indicate deviations below it. Vertical grey dotted lines indicate the identified breakpoints in each series. Coloured numbers denote statistically significant Mann-Kendall tau values ($p < 0.05$).

Therefore, microbialization of pelagic food webs plays a crucial role in shaping trophic dynamics[32], emphasising the need for a comprehensive understanding that goes beyond zooplankton to include broader community interactions and the role of organic matter in sustaining these processes.

Since most upwelling zones sustain rich fisheries and are consequently subject to high fishing pressure[10], the synergistic effects of fishing and climate change can undermine ecosystem resilience, impacting both population dynamics and the potential for recovery[21]. This trend is particularly evident in fish biomass, which responds rapidly to intense fishing pressure, often also leading to species loss and compromised ecosystem functions[21,41]. Importantly, the consistent nutrient supply in upwelling regions not only sustains high productivity, but also plays a critical role in maintaining ecosystem stability and resilience over time[1]. Disruptions in nutrient availability—whether through increases or decreases—can destabilise ecological equilibria, diminishing the capacity of these ecosystems to cope with the combined pressures of climate change and fishing intensity[1,8]. While the continuing cold waters may buffer some of the adverse impacts of warming, the combined effects of fishing on bottom-up processes within these ecosystems remain poorly understood, with strong implications for complex socioeconomic systems.

Although machine learning models, such as the Random Forest applied in this study, are inherently dependent on statistical patterns from the training dataset, we designed our modelling approach to minimise potential extrapolation errors. By using a long-term historical time series that includes periods of substantial environmental variability—such as La Niña events— we trained the model on a broad range of system states, which helps improve its generalisation capacity and reduces the likelihood of projecting outside its trained domain. The application of machine learning to climate projections has recently gained substantial support within climate science, emphasising that machine learning methods are good tools for advancing climate modelling[24], particularly in scenarios where complex system responses are difficult to capture using mechanistic models alone. Nevertheless, it is important to interpret these long-term projections with caution, especially under extreme warming scenarios that may introduce novel environmental regimes not fully represented in the historical data. Future studies that combine mechanistic and machine learning models could further enhance the robustness of these projections.

Online methods

Study area

Sampling occurred weekly from January 2005 to December 2016 in the upwelling system of Cabo Frio on the southeastern coast of Brazil (Fig. 1; 22°58'S, 42°00'W), as part of the Long-Term Ecological Research on the Cabo Frio Upwelling Systems (CFUS)[31]. This region is an important marine extractive reserve in the southwestern Atlantic Ocean, supporting both artisanal and commercial fisheries, and also under touristic pressure, leading to a myriad of ecosystem impacts. In addition to these human influences, upwelling events directly affect nutrient availability, contributing to high regional fluctuations in both biotic and abiotic components. Understanding how biological communities behave over time in such a dynamic environment is, therefore, a major challenge that can only be addressed through long-term monitoring programs and robust modelling approaches.

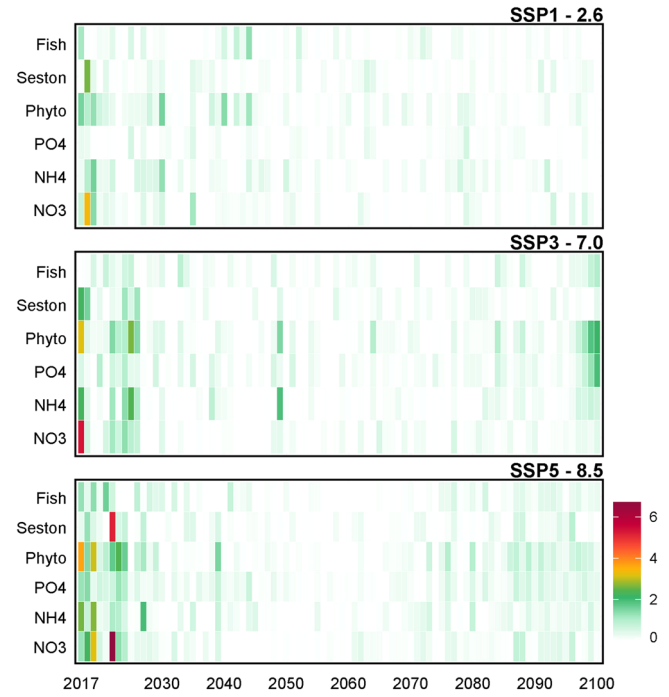

Fig. 5 | Annual magnitude of variation (average) under different scenarios. Darker colours indicate larger deviations from the historical average in Fish Caught, Seston biomass, Phytoplankton biomass, Phosphate, Ammonia, and Nitrate concentration.

Observational data and future warming scenarios

In the CFUS we sampled Sea Surface Temperature (SST°C); nutrients' concentration (i.e. nitrate, ammonia, and phosphate in micromolar); Chlorophyll-a (mg m^{-3}); seston (mg m^{-3}); and fishing data (catch amount in tonnes). We obtained weekly SST°C by using a Horiba multiparameter probe (Model U-5000; HGS No. 7JETA790). In addition, we obtained monthly SST°C projections between 2017 to 2100 for our study area, in an approximately 11 km^2 grid, from three Shared Socioeconomic Pathways (SSPs) of the Coupled Model Intercomparison Project Phase 6 (CMIP6) - NorESM2-MM model[24,42]. To validate the suitability of this model, we compared the SST projections with the ensemble median of all available CMIP6 models for the region. We found a strong correlation between the NorESM2-MM and the ensemble median across all scenarios, indicating that NorESM2-MM closely represents the central tendency of the multi-model ensemble and is not an outlier (Supplementary Fig. S9). This comparison supports the robustness of using NorESM2-MM as a representative model for regional SST trajectories in this study. The SSP scenarios represent alternative socio-economic pathways that society can follow and that can lead to different Representative Concentration Pathways (RCPs) based on radiative forcing levels of 2.6, 7.0 and 8.5 W m^{-2}. SSP1-2.6 represents a more sustainable scenario with low radiative forcing, leading to a global temperature increase of approximately 1.8 °C by the end of the century; SSP3-7.0 represents a high-challenge scenario with high radiative forcing, leading to a projected global temperature increase of around 3.6 °C by 2100; and SSP5-8.5 represents a more extreme scenario simulating a global temperature increase of about 4.4 °C[43].

We determined chlorophyll-a concentration by using a 3-L Niskin bottle at ~1-m deep. At the same moment, we sampled 2 litres of sub-superficial water, to estimate nutrients concentration. Both samples were then sent to the laboratory, where chlorophyll-a was first filtered using a 0.47 micrometre filter, and its absorbance was measured at different wavelengths using a spectrometer[44]; and nutrients concentration were extracted in a spectrophotometric Agilent UV-Vis Cary 60[45].

We used seston as a key variable representing the total particulate matter larger than 100 µm in the water column, including phytoplankton, micro and mesozooplankton, suspended organic particles, and detritus[46,47]. This variable provides a more integrated view of the trophic resource base available to planktivorous fish species. Seston biomass was sampled through three horizontal sub-superficial hauls. On each haul, a WP2 net with 100-micron mesh and 40 cm diameter was dragged for two minutes by a vessel at 2 knots speed. A flowmeter was attached to the mouth of the net for further calculation of the water volume filtered[48,49]. After each haul, the seston sample retained was stored and preserved in a 4% formalin solution diluted in seawater and previously buffered with sodium tetraborate (20g L^{-1}). In the laboratory, each sample was fractionated into two equal parts using the FolsomSplitter[50]. One part was weighed on a precision scale to obtain the wet weight (0.0001g). After this procedure, samples were dried in a greenhouse for 24 hours at approx. 60 °C to obtain the dry weight, which was used as seston biomass (SDB; mg m^{-3}).

We obtained annual fishing data (catch amount in tonnes) of primary fish consumers (i.e., *Mugil* spp., *Opisthonema oglinum, Sardinella brasiliensis*) for the period January 2005 to December 2015 from literature based on landing reconstructions[51]. This reconstruction was modelled based on official information provided by municipalities in our study region. To obtain monthly fishing estimates, necessary to relate to seston biomass, we used data from January 2016 to December 2023 provided by 'Fundação Instituto de Pesca de Arraial do Cabo' (FIPAC). We then calculated monthly proportions (tonnes $month^{-1}$) from this recent data and applied these proportions to the annual values for the period 2005-2016 to estimate monthly catches for these years. This approach allowed us to derive a consistent monthly fishing dataset from January 2005 to December 2016 (Supplementary Fig. 10).

Prior to modelling, all observational time series were subjected to a common data pre-processing workflow. We first applied a normal distribution to eliminate values outside the 99% confidence interval within each variable. The missing values resulting from this procedure and sampling gaps (*ie. max of 63 values for NO_3 from a total of 627 samples*) were then estimated using the "rfImpute" function from the "randomForest" package[52]. This function estimates missing values for explanatory variables as a function of the response variable based on weighted averages. The weights are measures of similarity, determined by how frequently two samples end up in the same "leaf" over 999 trees. We validated this procedure using the mean squared residual (MSR) and the proportion of explained variance (%Var), where a lower MSR and a higher %Var indicate better predictions. We then applied a moving average (k = 4 weeks to Nutrients, Phyto and Seston carbon; and k = 1 month to fish biomass) to smooth short-term fluctuations and reduce noises in the data, making it easier to identify and highlight more robust long-term trends.

Ecosystem modelling

To project ecosystem responses to nutrients availability and warming up to the end of the century we developed a framework based on supervised Random Forest regression models using a walk-forward validation approach. This framework is based on the "randomForest" function from the randomForest package. It allowed us to understand the model's performance over time by iteratively training the model on sequential segments of the time series data and testing predictions on subsequent data samples. Each iteration involves training the Random Forest on the training dataset with 999 trees and considering the total number of explanatory variables minus the lagged variables (see below) as candidates at each split (mtry). The model's performance (%Var and MSR) and validation metrics (RMSE and MAE) are then evaluated on the train and test datasets, respectively. This process is repeated for a predefined number of steps, which varies from model to model according to the best results achieved (please refer to Supplementary Material to check all performance and validation results for all models).

Due to temporal dependencies in time series data—where past values can influence future values—we introduced a lag to the explanatory

variables, helping the model to use past information to better predict future outcomes. The amount of lag was measured in 4 weeks to Nutrients, Phytoplankton and Seston carbon and 1 month to fish biomass; and determined based on the best performance metrics for each model. In addition to adjusting the response variables (nutrients, phytoplankton, seston and fish biomass) in the historical data, at each iteration, the function also runs predictions using model outputs and future-modelled explanatory variables, such as SST values from the CMIP6 warming scenarios. Since Random Forest models depend on a series of random decision trees, which can generate different values within each run, we run each model 100 times and calculate the average of all metrics generated by the function, thus achieving more precise predictions. Considering potential uncertainty propagation across sequential models, we assessed prediction variability using bootstrap-derived standard deviations (Supplementary Table 2).

We first run the above-explained framework to model the Sea Surface Temperature (°C) dependence of the three crucial nutrients: Nitrate (NO_3), Ammonia (NH_4) and Phosphate (PO_4). We evaluated the relationship between in situ SST and SST anomalies and found a strong correlation ($R > 0.74$), indicating that both metrics capture the dominant variability associated with upwelling dynamics. Because absolute SST preserves information about the thermal state of the system and is widely used in ecological and oceanographic studies[53], it was selected as the predictor variable for model development. This procedure resulted in weighted adjusted values and future predictions based on the CMIP6 warming scenarios. We then related the adjusted nutrient values from these models to estimate the scaling of Chlorophyll-a, thereby understanding how these bioenergetic processes favour primary production over time, following the Eq. (1):

$$\begin{aligned} NO_{3,adj} &= NO_3 \sim SST + lag_9(SST) \\ NH_{4,adj} &= NH_4 \sim SST + lag_4(SST) \\ PO_{4,adj} &= PO_4 \sim SST + lag_4(SST) \\ CHLa_{adj} &= CHLa \sim NO_{3,adj} + NH_{4,adj} + PO_{4,adj} \\ &\quad + \mathrm{SST} + \mathrm{lag}_4(NO_{3,adj} + NH_{4,adj} + PO_{4,adj} + \mathrm{SST}) \end{aligned} \tag{1}$$

To improve predictions of consumers dependence on production in the food web, we transformed the adjusted Chlorophyll-a biomass ($CHLa_{adj}$) into phytoplankton carbon (PC_T) by assuming a natural log scale and positive relationship following the Eq. (2)[54]:

$$\ln PC_T = \ln (268 \cdot CHLa_{adj}^{\,0.64}) \tag{2}$$

We converted the seston biomass into seston carbon using a conversion factor[55] (Q) of 0.6, to model the response of seston carbon to variations in phytoplankton carbon and sea-surface temperature, following the Eq. (3):

$$\ln SC_T = \ln (SDB \cdot Q) \sim \ln (PC_T) + SST + \mathrm{lag}_4(\ln (PC_T) + SST) \tag{3}$$

We then assumed a logarithmic scale dependence between the monthly biomass of primary consumer fishes and the average monthly carbon biomass of seston and temperature, following the Eq. (4):

$$\ln F_{adj} = \ln F \sim \ln SC_T + SST + \mathrm{lag}_1(SC_T + SST) \tag{4}$$

Model validation

All models were validated using a walk-forward approach with an expanding training window. This method iteratively trains the model on all available data from the start of the time series up to a certain point (from observation 1 to i + steps). The model is then evaluated on the immediately subsequent, unseen block of observations (the test window). This test window moves forward one step at a time alongside the expanding training data. At each step, predictions are generated for this test window, and model performance is quantified using Mean Absolute Error (MAE), calculated as the average absolute difference between predicted and observed values, and Root Mean Square Error (RMSE), calculated as the square root of the mean of the squared differences. Both metrics are expressed in the same units as the response variable, so lower values indicate better predictive performance. This procedure rigorously tests the model's ability to generalize to future data while leveraging the entire available history for training, allowing for a robust assessment of how well it tracks temporal dynamics throughout the entire dataset.

To further assess the model's generalizability and stability, we conducted a complementary validation with an independent dataset. This involved iteratively training the model on sequential windows between 2005–2014 (train data) and validating its predictions each time on the same, fixed independent test set (2015–2016). Predictive accuracy was also quantified by using MAE and RMSE (see results in Supplementary Figs. 11 and 12).

Trend analysis

To mitigate the impact of seasonality on the projected trends, we first standardised monthly values within each scenario by calculating the *z*-score (i.e., subtracting the monthly mean and dividing by the monthly standard deviation for each scenario and month). This approach allowed us to remove the seasonal cycle and highlight long-term trends. The standardised anomalies were then smoothed using a Loess regression (span = 0.75) to reduce short-term fluctuations and emphasise the underlying trend over time for all the variables (i.e. NO3 to Fish Biomass). Finally, annual averages of the standardised values were calculated to facilitate the visualisation of temporal patterns. We then conducted a Mann-Kendall test in which context, negative values indicate a decreasing trend over time, while positive values indicate an increasing trend. Recognising that the Mann-Kendall test can be influenced by autocorrelation, we also performed a pre-whitened Mann-Kendall test for comparison. Additionally, we employed a bootstrap method to estimate the error associated with the Tau values (please see Supplementary Table 1 for the results).

To assess potential structural changes in these trends, we applied breakpoint analysis. The minimum segment size (h) was set to 20% of the total observations to ensure sufficient data for detecting meaningful breaks. Breakpoints were visually inspected through plots and summarised to identify significant shifts in trends across the scenarios. The number of breakpoints selected for each variable was based on the intersection of Bayesian Information Criterion (BIC) and Residual Sum of Squares (RSS) metrics. We also calculated the annual average magnitude of variation by standardising monthly values through subtraction of the monthly mean and division by the monthly standard deviation. The squared mean of these standardised magnitudes was then computed for each variable, scenario, and year to capture the annual variation in relative magnitude. All analyses and graphics were performed using R software version 4.2.2[56].

Reporting summary

Further information on research design is available in the Nature Portfolio Reporting Summary linked to this article.

Data availability

All data necessary to reproduce the analyses and results of this study are publicly available on the Zenodo repository at https://doi.org/10.5281/zenodo.14592869 [84].

Code availability

All custom R scripts used to generate, process, and analyse the data in this study are publicly available on the Zenodo repository at https://doi.org/10.5281/zenodo.14592869, with no restrictions to access. Analyses were conducted using R version 4.2.2 (R Core Team, 2022).

Received: 25 March 2025; Accepted: 3 March 2026;
Published online: 19 March 2026

References

1. Moore, C. et al. Processes and patterns of oceanic nutrient limitation. *Nature Geosci* **6**, 701–710 (2013).
2. Bruno, J. F., Carr, L. A. & O'Connor, M. I. Exploring the role of temperature in the ocean through metabolic scaling. *Ecology* **96**, 3126–3140 (2015).
3. Capitani, L., Araujo, J. N., Vieira, E. A., Angelini, R. & Longo, G. O. Ocean warming will reduce standing biomass in a tropical Western Atlantic reef ecosystem. *Ecosystems* **25**, 843–857 (2022).
4. Barneche, D. R. et al. Warming impairs trophic transfer efficiency in a long-term field experiment. *Nature* **592**, 76–79 (2021).
5. Audzijonyte, A. et al. Fish body sizes change with temperature but not all species shrink with warming. *Nat. Ecol. Evol.* **4**, 809–814 (2020).
6. Rosa, J. C. L. et al. Seasonal changes in the size distribution of copepods is affected by coastal upwelling. *Diversity* **15**, 637 (2023).
7. Nunes, L. T. et al. Predicting the effects of body size, temperature and diet on animal feeding rates. *Funct Ecol* **35**, 2229–2240 (2021).
8. Fuchs, H. L. & Franks, P. J. S. Plankton community properties determined by nutrients and size-selective feeding. *Mar. Ecol. Prog. Ser.* **413**, 1–15 (2010).
9. Meunier, C. L. et al. Nutritional thermal ecology: investigating the combined influence of temperature and nutrient availability on plant ectotherm trophic interactions. *Oikos* **2024**, e10940 (2024).
10. Pauly, D. & Christensen, V. Primary production required to sustain global fisheries. *Nature* **374**, 255–257 (1995).
11. Zhurbas, V., Laanemets, J. & Nyman, E. Modeling of the mesoscale structure of coupled upwelling/downwelling events and the related input of nutrients to the upper mixed layer in the Gulf of Finland, Baltic Sea. *J. Geophys. Res.* **113**, C05004 (2008).
12. Fernandes, L. D. de A., Fagundes-Netto, E. B. & Coutinho, R. Inter-annual cascade effect on marine food web: A benthic pathway lagging nutrient supply to pelagic fish stock. *PLoS ONE* **12**, e0184512 (2017).
13. Xiu, P., Chai, F., Curchitser, E. N. & Castruccio, F. S. Future changes in coastal upwelling ecosystems with global warming: The case of the California Current System. *Sci. Rep.* **8**, 2866 (2018).
14. Du, T. et al. Future changes in coastal upwelling and biological production in eastern boundary upwelling systems. *Nat. Commun.* **15**, 6238 (2024).
15. Sommer, U., Peter, K. H., Genitsaris, S. & Moustaka-Gouni, M. Do marine phytoplankton follow Bergmann's rule sensu lato? *Biol. Rev.* **92**, 1011–1026 (2017).
16. Fahui, G. et al. Spatial shifts in size structure, phylogenetic diversity, community composition and abundance of small eukaryotic plankton in a coastal upwelling area of the northern South China Sea. *J. Plankton Res.* **42**, 650–667 (2020).
17. Ware, D. M. & Thomson, R. E. Bottom-Up ecosystem trophic dynamics determine fish production in the Northeast Pacific. *Science* **308**, 1280–1284 (2005).
18. Frank, K. T., Petrie, B., Shackell, N. L. & Choi, J. S. Reconciling differences in trophic control in mid-latitude marine ecosystems. *Ecol. Lett.* **9**, 1096–1105 (2006).
19. Chassot, E., Mélin, F., Pape, O. L. & Gascuel, D. Bottom-up control regulates fisheries production at the scale of eco-regions in European seas. *Mar. Ecol. Prog. Ser.* **343**, 45–55 (2007).
20. Conti, L. & Scardi, M. Fisheries yield and primary productivity in large marine ecosystems. *Mar. Ecol. Prog. Ser.* **410**, 233–244 (2010).
21. Blanchard, J. L. et al. Potential consequences of climate change for primary production and fish production in large marine ecosystems. *Phil. Trans. R. Soc. B* **367**, 2979–2989 (2012).
22. Jochum, M., Schneider, F. D., Crowe, T. P., Brose, U. & O'Gorman, E. J. Climate-induced changes in bottom-up and top-down processes independently alter a marine ecosystem. *Phil. Trans. R. Soc. B.* **367**, 2962–2970 (2012).
23. Fujita, K. et al. Increase in fish production through bottom-up trophic linkage in coastal waters induced by nutrients supplied via submarine groundwater. *Front. Environ. Sci.* **7**, 82 (2019).
24. Eyring, V. et al. Overview of the Coupled Model Intercomparison Project Phase 6 (CMIP6) experimental design and organization. *Geosci. Model Dev.* **9**, 1937–1958 (2016).
25. NOAA, National Centers for Environmental Information. Monthly Global Climate Report for Annual 2011. (2012). https://www.ncei.noaa.gov/access/monitoring/monthly-report/global/201113.
26. Reynolds, C. S. Ecology of Phytoplankton. In: Usher, M., Saunders, D., Peet, R., Dobson, A., eds. Ecology, B: Cambridge University Press, 551p, (2006).
27. Echevin, V. et al. Physical and biogeochemical impacts of RCP8.5 scenario in the Peru upwelling system. *Biogeosciences* **17**, 3317–3341 (2020).
28. Chust, G. et al. Biomass changes and trophic amplification of plankton in a warmer ocean. *Glob. Chang. Biol.* **20**, 2124–2139 (2014).
29. Heneghan, R. F., Everett, J. D., Blanchard, J. L., Sykes, P. & Richardson, A. J. Climate-driven zooplankton shifts cause large-scale declines in food quality for fish. *Nat. Clim. Chan.* **13**, 470–477 (2023).
30. Barange, M. et al. Impacts of climate change on marine ecosystem production in societies dependent on fisheries. *Nat. Clim. Chang.* **4**, 211–216 (2014).
31. Matos, T. S. et al. Early warning indicators of decadal shifts in the planktonic assemblage of the Cabo Frio upwelling ecosystem. *Ecol. Indic.* **167**, 112674 (2024).
32. Haas, A. F. et al. Global microbialization of coral reefs. *Nat. Microbiol.* **1**, 16042 (2016).
33. Kirchman, D. L. Processes in microbial ecology. Oxford University Press. (2018).
34. Campelo, R. P. S. et al. Zooplankton biomass around marine protected islands in the tropical Atlantic Ocean. *J. Sea Res.* **154**, 101810 (2019).
35. Kwiatkowski, L. et al. Twenty-first century ocean warming, acidification, deoxygenation, and upper-ocean nutrient and primary production decline from CMIP6 model projections. *Biogeosciences* **17**, 3439–3470 (2020).
36. Azam, F. et al. The ecological role of water-column microbes in the sea. *Mar. Ecol. Prog. Ser.* **10**, 257–263 (1983).
37. Coma, R., Ribes, M., Gili, J. M. & Hughes, R. N. The ultimate opportunists: consumers of seston. *Mar. Ecol. Prog. Ser.* **219**, 305–308 (2001).
38. Dias, C. O., Bonecker, A. C. T., Carvalho, P. F., Paranhos, R. & Bonecker, S. L. C. Seston biomass in plankton assemblages in the Southwestern Atlantic Ocean: spatial, vertical, and temporal variations. *An. Acad. Bras. Cienc.* **96**, e20230490 (2024).
39. Skinner, C. Offshore pelagic subsidies dominate carbon inputs to coral reef predators. *Sci. Adv* **7**, eabf3792 (2021).
40. Fanelli, E. et al. The pelagic food web of the Western Adriatic Sea: a focus on the role of small pelagics. *Sci. Rep.* **13**, 14554 (2023).
41. Scherer, M. E. G. et al. Under pressure: an integrated assessment of human activities and their potential impact on the ecosystem components of the Southern Brazilian continental shelf. *npj Ocean Sustain* **3**, 9 (2024).
42. Copernicus Climate Change Service, Climate Data Store. CMIP6 climate projections. Copernicus Climate Change Service (C3S) Climate Data Store (CDS) (2021).
43. Vuuren, D. P. V. et al. The representative concentration pathways: an overview. *Climatic Change* **109**, 5–31 (2011).

44. Thrane, J.-E. et al. Spectrophotometric analysis of pigments: A critical assessment of a high-throughput method for analysis of algal pigment mixtures by spectral deconvolution. *PLoS ONE* **10**, e0137645 (2015).
45. Strickland, J. & Parsons, T. A practical handbook of seawater analysis (2nd ed.). Ottawa: Fisheries Research Board of Canada Bulletin 310 pp (1972).
46. Gladstone-Gallagher, R. V., Lohrer, A. M., Lundquist, C. J. & Pilditch, C. A. Effects of detrital subsidies on soft sediment ecosystem function are transient and source dependent. *PLoS One* **11**, e0154790 (2016).
47. Huguet, C. Seston quality and available food: importance in the benthic biogeochemical cycles. In: Rossi S, Bramanti L, Gori A & Orejas C (Eds), Marine Animal Forests, Cham.: Springer Verlag, p. 1–27 (2015).
48. Álvarez, E., López-Urrutia, Á, Nogueira, E. & Fraga, S. How to effectively sample the plankton size spectrum? A case study using FlowCAM. *J. Plankton Res.* **33**, 1119–1133 (2011).
49. Álvarez, E., Moyano, M., López-Urrutia, Á, Nogueira, E. & Scharek, R. Routine determination of plankton community composition and size structure: a comparison between FlowCAM and light microscopy. *J. Plankton Res.* **36**, 170–184 (2014).
50. Boltovskoy, D. C. Atlas de zooplancton del Atlántico sudoccidental: y métodos de trabajo con el zooplancton marino. Mar del Plata: Argentina, 936 pp (1981).
51. Freire, K. M. F. et al. Reconstruction of marine commercial landings for the Brazilian industrial and artisanal fisheries from 1950 to 2015. *Front. Mar. Sci.* **8**, 659110 (2021).
52. Liaw, A. & Wiener, M. Classification and Regression by randomForest. *R News*, 18–22 (2002).
53. Calado, L., Gangopadhyay, A., Watanabe, W. B. & Silveira, I. C. A. Mushroom-like eddy dipoles in the Brazil Current: Formation and mesoscale dynamics. *Reg. Stud. Mar. Sci.* **90**, 104414 (2025).
54. Sathyendranath, S. et al. Carbon-to-chlorophyll ratio and growth rate of phytoplankton in the sea. *Mar. Ecol. Prog. Ser.* **383**, 73–84 (2009).
55. Postel, L., Fock, H. & Hagen, W. Biomass and abundance. In: Harris RP, Wiebe PH, Lenz J, Skjoldal HR, Huntley M, eds. ICES Zooplankton Methodology Manual. San Diego: Academic Press, 684pp, (2000).
56. R Core Team. R: A language and environment for statistical computing. R Foundation for Statistical Computing, Vienna, Austria (2022).

Acknowledgements

We thank the World Climate Research Programme for producing and making available the CMIP6 model output, the Earth System Grid Federation (ESGF) for archiving the data and providing access, and the multiple funding agencies who support CMIP6 and ESGF. We are grateful to the team of the Chemistry Division of the Institute of Sea Study Admiral Paulo Moreira (IEAPM) for nutrient analysis. We thank all the researchers and military personnel from IEAPM which contributed to data sampling over the years. We thank the Arraial do Cabo Fishing Institute Foundation (FIPAC) for the fishing data provided. This project has received funding from the European Union's Horizon 2020 research and innovation programme under Grant Agreement No 862428 (MISSION ATLANTIC). This output reflects only the author's view and the Research Executive Agency (REA) cannot be held responsible for any use that may be made of the information contained therein.

Author contributions

L.T.N. conceived the study, designed the methodology, conducted the data analysis, and wrote the first draft of the manuscript. T.S.M. conceived the study, designed the methodology, performed the laboratory analyses, and contributed to writing the first draft. C.R. contributed to interpretation of results, writing the first draft and revising the manuscript. Y.A. contributed to study design, interpretation of results, and manuscript revision. G.C. contributed to interpretation of results and manuscript revision. A.C. performed the laboratory analyses and contributed to manuscript revision. R.C. contributed to study design and manuscript revision. C.E.L.F. contributed to study design and manuscript revision. P.M. contributed to study design and manuscript revision. L.F. conceived the study, designed the methodology, supervised the research, and contributed to writing and revising the manuscript. All authors approved the final version of the manuscript.

Competing interests

The authors declare no competing interests.

Additional information

Supplementary information The online version contains supplementary material available at https://doi.org/10.1038/s43247-026-03395-1.

Correspondence and requests for materials should be addressed to Lucas T. Nunes.

Peer review information . *Communications Earth and Environment* thanks the anonymous reviewers for their contribution to the peer review of this work. Primary Handling Editors: Michael Stukel and Alice Drinkwater. A peer review file is available.